fortune Journals

Research Article

JOURNAL OF ANALYTICAL TECHNIQUES AND RESEARCH

ISSN: 2687-8038

Enhanced Oxygen Tolerance in CO2 Electroreduction to Formic Acid on SnO2/CN Catalyst through Alkali-Heat Treatment

Mingxue Su[1,2], Zhenguo Guo[3], Ning Li[1,2*] and Bing Zhua[2]

Abstract

The electro-reduction of carbon dioxide (eCO_2RR) to formic acid (HCOOH) is very selective while employing the composite catalyst tin oxide/carbon nitride (SnO_2/CN). However, the abundance of O_2 and the minimal level of CO_2 in industrial exhaust gases prevent the catalyst's electrocatalytic activity. The current study employs alkali-heat intervention in the CN payload manufacturing process to increase the electrocatalytic yield and O_2 tolerance of SnO_2/CN. XPS spectroscopy found that alkali-heat therapy enhances CO_2 adsorption and raises the alkaloid level of composite catalyst by revealing a greater percentage of CN's surface amino groups. The improved metal-support contact allowed electrons to flow from the nitrogen of alkali heated CN to tin (Sn), resulting in exceptionally electron-rich Sn species nuclei that facilitated CO_2 activation and reduction. A CO_2 temperature-designed desorption study showed that the catalyst and CO_2 bond more strongly after alkali-heat treatment. A multi-component competitive adsorption curve study indicated more advantages to the alkali-heat process for CO_2/O_2 separation. Electrolytic studies demonstrated a faradaic efficiency (FE) of 90.5% for HCOOH at a potential of -1.5V (vs. Ag/AgCl) after two hours with alkali heated SnO_2/CN. Even in the presence of simulated industry exhaust gas FEHCOOH was 69.4%, showing greater oxygen endurance than untreated SnO_2/CN.

Keywords: CO_2; HCOOH; g-C_3N_4; SnO_2; Alkali-heat treatment.

Introduction

When compared to photo-reduction and thermal-reduction, electro-reduction offers a simpler and more environmentally friendly method for producing high-value chemicals and reducing CO_2 emissions, studied by [1]. The compound formic acid (HCOOH), a product of CO_2 electro-reduction, serves as a versatile feedstock for various useful chemicals and a hydrogen fuel storage medium [2]. Economically, formic acid outperforms various competitors such as CO, CH_3OH, C_2H_4, and $CH_3CH_2CH_2OH$ [3]. Several metallic elements, metal oxides, and composites have been used for CO_2 electro-reduction, with tin dioxide (SnO_2) showing a higher selectivity towards HCOOH [4-6]. An endeavor fostered to improve the stimulating efficiency of SnO_2, and the integration with an N-doped carbon (CN) substrate is considered satisfactory [7, 8]. However, [4] implied the nitrogen doping procedure for CN is commonly complex and involves external nitrogen sources. Graphite-like carbon nitride (g-C_3N_4), a nitrogen-rich material, provides a more regulated procedure for preparation [9, 10]. Current research has presented g-C_3N_4 as a catalyst support in electrocatalytic systems [11-13]. The amino groups and pyridinic N species in g-C_3N_4 can anchor acidic

Affiliation:

[1]Hefei Cement Research and Design Institute Corporation Ltd, Hefei, 230022, Anhui, China

[2]Anhui Key laboratory of Green and Low-carbon Technology in Cement Manufacturing, Hefei, 230022, Anhui, China

[3]School of Chemistry and Chemical Engineering, Hefei University of Technology, Hefei, 230009, Anhui, China

***Corresponding author:**
Ning Li, Hefei Cement Research and Design Institute Corporation Ltd, Hefei, 230022, Anhui, China

And Anhui Key laboratory of Green and Low-carbon Technology in Cement Manufacturing, Hefei, 230022, Anhui, China.

Citation: Mingxue Su, Zhenguo Guo, Ning Li and Bing Zhu. Enhanced Oxygen Tolerance in CO2 Electroreduction to Formic Acid on SnO2/CN Catalyst through Alkali-Heat Treatment. Journal of Analytical Techniques and Research. 6 (2024): 19-27.

Received: February 01, 2024
Accepted: February 07, 2024
Published: February26, 2024

Mingxue Su, et al., J Anal Tech Res 2024
DOI:10.26502/jatr.41

CO_2 to benefit the CO_2 reduction reaction (CO_2RR) [14], making it a cost-effective CN carrier without the need for amino group grafting. Most CO_2 electro-reduction researches have been conducted under pure CO_2 conditions, neglecting challenges posed by low CO_2 concentrations in the industry exhaust gas [15]. Creating a localized enhancement of a CO_2 microenvironment surrounding the electrocatalyst becomes crucial [16]. Amino groups, through Lewis acid-base interactions, provide CO_2 adsorption sites and enhance CO_2 electro-reduction kinetics [17-19]. g-C_3N_4, with its inherent amino functional groups, can potentially improve precise surface area and electron transfer capability through alkali and hydrothermal treatment [20], making it an ideal electrocatalyst support for direct industry exhaust gas electro-reduction. In this study, the g-C_3N_4 support was exposed to metallic and alkali-heat ablation. Our primary focus was on determining their impact on electron transfer capabilities and CO_2 adsorption/activation at active Sn sites. In addition, we investigated the electrochemical performance of the SnO_2/g-C_3N_4 catalyst under pure CO_2 gas flow and simulated industry exhaust gas (SIEG) to assess both oxygen sensitivity and electrocatalytic efficacy.

Material and Methods

Materials

The Sinopharm Chemical Reagent Company of China provided us with melamine (CP), potassium hydroxide (KOH, AR), alcohol (AR), and tin (II) chloride. Toray (Japan) supplied the sheet of carbon paper. Nafion solution (5wt%) and Nafion 117 membrane were obtained from DuPont (USA). All substances have been used as received, with no further modifications.

Catalyst preparation

The formation of g-C3N4 included a thermal polymer of melamine at 550°C, with a rate of heating of 10°C per minute in a covered container for two hours in an air atmosphere. The resulting yellow substance was then crushed into a powder after cooling and given the designation CN.

1g of CN was immersed in 20 mL of 0.1 M of KOH solution. The product was obtained by centrifugation after three hours of stirring, followed by a deionized (DI) water wash and overnight drying at 75°C. This material was marked as CNOH.

Similar to CNOH, with an additional step of heating the solid at 550°C in a covered beaker in dynamic air for one hour after centrifugation. Following the cooling process, the solution evaporated overnight at 75°C after being rinsed with dehydrated water. The tag for this substance was CNOHHT. A study by [21] found that SnO_2/g-C_3N_4 composite catalysts has been generated using a new method based on prior research. A standard solution utilized 80 milliliters of ethanol to scatter 0.38 grams of $SnCl_2$ and 0.5 grams of CN (CNOH or CNOHHT). After one hour of stirring, the mixture was reflux for one hour at 100°C. The final product was collected, let to cool to room temperature, purified with DI water, then left to dry at 70°C instantaneously. SnO_2/CN, SnO_2/CNOH, and SnO_2/CNOHHT were the final product identities.

Identification of materials

Materials were investigated using a Smart Lab X-ray diffractometer made by Smart Labs (in Japan) with a Cu-Kα source to obtain powder XRD patterns. Materials were analyzed for CO_2-TPD using a ChemStar TPx chemisorption analyzer (Quantachrome Instrument, USA). The functional chemicals in each sample were identified using Fourier transform infrared spectroscopy (FTIR) on a ThermoFisher Nicolet IS20 instrument (United States), using KBr disks for analysis. Materials' X-ray photo electron spectra (XPS) were collected using a Thermo ESCALAB 250 (U.S.A) and a monochromate Al Kα X-ray source. The textural characteristics of the materials were investigated using an Autosorb Q instrument (Quanta chrome).

Preparation of functional electrodes

Initially, 10 milligrams of SnO_2/CN (SnO_2/CNOH or SnO_2/CNOHHT) were submerged in 1 milliliter of alcohol with 100 µl of Nafion solution. The combo was ultrasonically treated for 30 minutes to ensure appropriate dispersion and homogeneous coating. The resulting mixture was then applied to a carbon paper substrate with a spray cannon. The process of pouring on the carbon paper was repeatedly processed before it reached the desired amount of 1 mg/cm^2. The result was selected as a functioning electrode.

Electrochemical experimentations

Electrochemical studies were conducted using a CHI-760E electrochemical computer (Shanghai Chenhua Instruments Company, China). The Nafion 117 membrane separated the cathodic and anodic chambers. The functional and standard electrodes (Ag/AgCl) were in the cathodic area, with the counter electrode (Pt sheet) in the anode chamber. The electrolyte used was a 0.5 M $KHCO_3$ solution. Before those studies, high-purity CO_2 was given for at least 30 minutes. The linear sweep voltammetry (LSV) studies were performed at the scanning speed of 50 mV/s, spanning -2.1 and zero volts (against Ag/AgCl). Electrochemical impedance spectroscopy (EIS) has been done at low rates (0.01 Hz) and at elevated speeds (100 kHz), with an amplitude of 5 mV at an open circuit voltage. Stability testing was conducted using chronoamperometry with an electrolytic setting of -1.5 V vs. Ag/AgCl. Gas products were detected by gas chromatography (GC, Thermo Trace 1310, USA) with flame ionization detector (FID) and thermal conductivity

Mingxue Su, et al., J Anal Tech Res 2024
DOI:10.26502/jatr.41

(TCD). Ion chromatography (IC, Metrohm Eco, Switzerland) was used for analyzing liquid products. The FEHCOOH is determined utilizing a formula (1):

$$FE = \frac{2 \times n \times F}{Q} \times 100\% \quad (1)$$

In this context, 'n' indicates the proportion of formic acid per mol, 'F' indicates the Faradaic constant (96485 C/mol), and 'Q' represents the galvanic charge in C.

The FE of CO and H_2 were determined using the formula (2):

$$FE = \frac{10^{-3} \times 2 \times v\%FG}{60RTI} \times 100\% \quad (2)$$

The indication "v%" shows the CO concentration or H_2 in the measured gas. 'G' denotes the CO_2 rate of flow (10 ml/min), 'R' the gas constant (8.314 J/mol/K), 'T' the temperature (298 K), and 'I' the constant current.

Results and Discussion

The crystallographic phases found in each sample were identified by the XRD spectrum. Figure1 shows three different peak angles at 26.6°, 33.8°, and 51.7°, signifying (110), (101), and (211) facets of SnO_2, respectively studied by [22]. The modest but clear spectra at 27.7° are characterized to (002) interlayer showing CN's graphitic-like composition. Significantly, the highest intensities at 27.7° for SnO_2/CNOH and SnO_2/CNOHHT were lower and wider than those for SnO_2/CN. [23] shows a decrease in the in-plane compositional loading pattern of CN following alkali and alkali-heat therapies.

The textural attributes of every sample are summarized in Table 1. The aggregate volume of pores remained constant throughout all samples. SnO_2/CN had a BET surface area of 9.98 m^2/g, which was much lower than 11.18 m^2/g of SnO_2/CNOH but higher than 9.66 m^2/g of SnO_2/CNOHHT. The inclusion of alkali can lead to deterioration of the C layer, raising the specific region of C-containing compounds. Alkali-heat ablation can produce structural collapse in C-based materials, leading to a decline in an exact surface region.

Table 1: Textural characteristics of each material

Samples	BET surface area (m^2/g)	Total pore volume (ml/g)
SnO_2/CN	9.98	0.073
SnO_2/CNOH	11.18	0.07
SnO_2/CNOHHT	9.66	0.072

As displayed in Figure 2, the FTIR analysis displays the molecular framework of all materials. The area at 811 cm-1 corresponds to the triazine unit. The peaks at 1100 cm-1 and 1600 cm-1 are due to the typical resonance of C-N and C≡N patterns. The spectra at 3179 cm-1 and 3269 cm-1 represent the vibratory stretching of -NHx. Each sample contains such distinct peaks, indicating the preservation of CN's distinctive compositional component. SnO_2/CNOHHT exhibits unique bands at 2175 cm-1, similar to metal-doped CN materials [20]. This indicates the potential for potassium to be attached to CN through heat treatment.

All materials under investigation were thoroughly analyzed in terms of their compositions and chemical states using profiles obtained from X-ray photoelectron spectroscopy (XPS). Tin 3d3/2 and Tin 3d5/2 have been recognized as two distinct bands in Figure3 at about 487 and 496 electron volts, respectively. This indicates that Sn^{4+} of SnO_2 are present across each of materials. The O 1s spectra of O^{2-} and oxygen absorbed are shown in Figure4 at exactly 530 and 532 electron volts, respectively. Three peak levels, located at approximately 398 eV, 399 eV, and 401 eV in Figure5, are indicative of amino chains, tertiary N

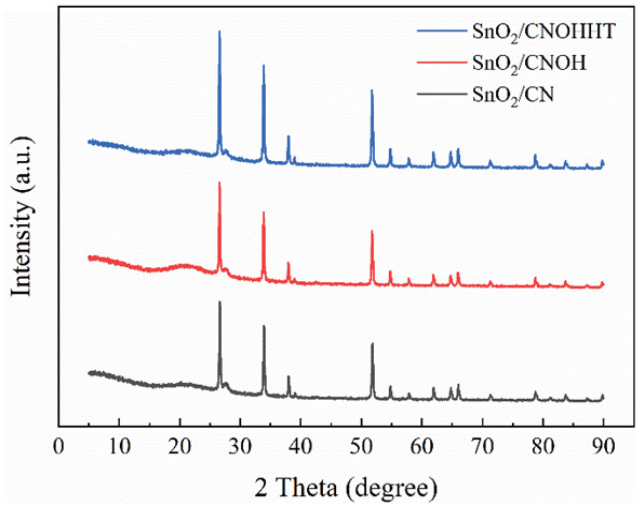

Figure 1: XRD patterns of all the samples

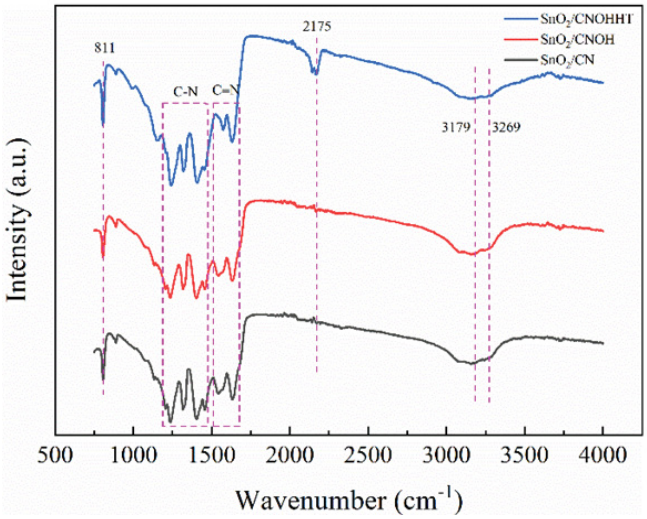

Figure 2: FTIR spectrums of all the samples

Citation: Mingxue Su, Zhenguo Guo, Ning Li and Bing Zhu. Enhanced Oxygen Tolerance in CO2 Electroreduction to Formic Acid on SnO2/CN Catalyst through Alkali-Heat Treatment. Journal of Analytical Techniques and Research. 6 (2024): 19-27.

Mingxue Su, et al., J Anal Tech Res 2024
DOI:10.26502/jatr.41

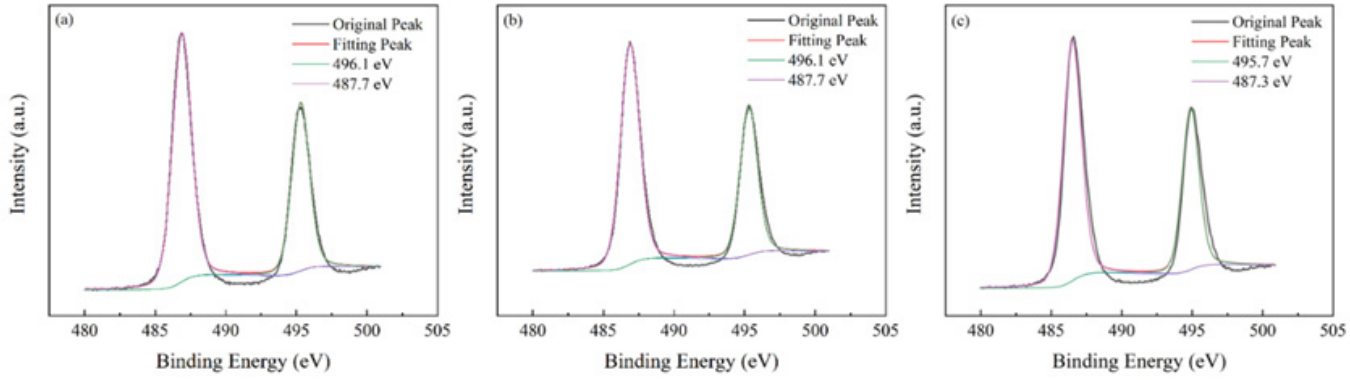

Figure 3: High-resolution Sn 3d XPS spectra of (a) SnO_2/CN, (b) SnO_2/CNOH and (c) SnO_2/CNOHHT

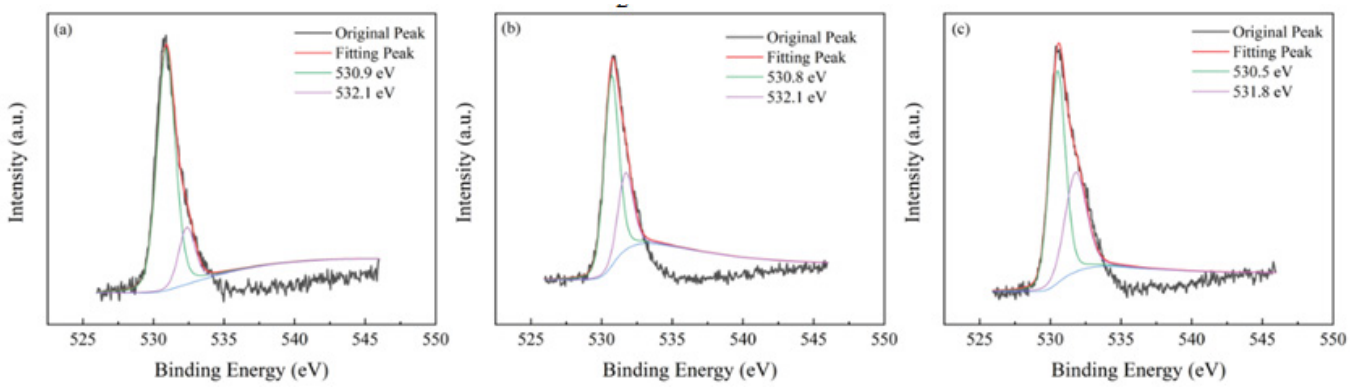

Figure 4: High-resolution O 1s XPS spectra of (a) SnO_2/CN, (b) SnO_2/CNOH and (c) SnO_2/CNOHHT

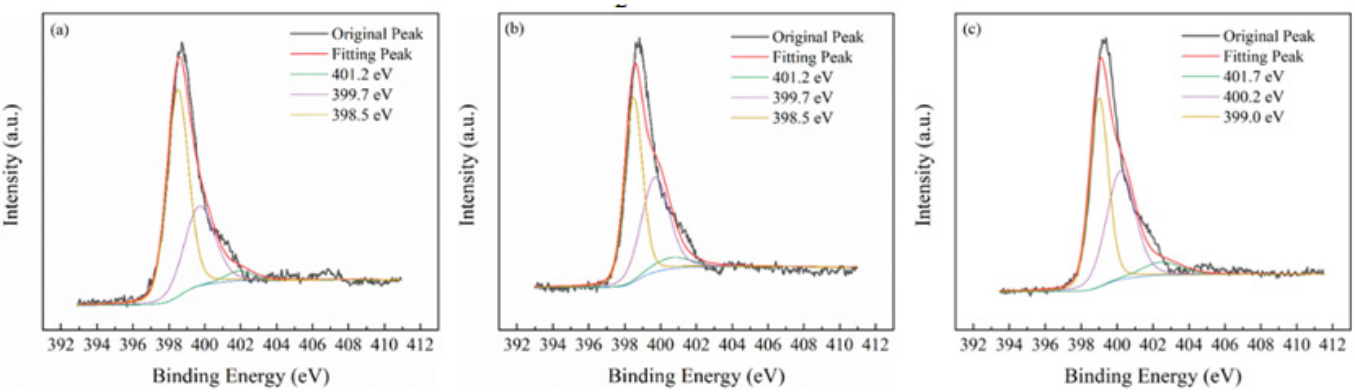

Figure 5: High-resolution N 1s XPS spectrum of (a) SnO_2/CN, (b) SnO_2/CNOH and (c) SnO_2/CNOHHT

groups, and sp2 polarized N atoms in the CN substrate [24]. All species of nitrogen are provided in Table 2. The amino groups' peak region increased to 7% for SnO_2/CNOHHT from 3.7% for SnO_2/CN, showing that alkali and alkali-heat interventions may significantly raise the amount of surface amino bonds in CN. The rise in surface amino groupings improves the catalyst's alkalinity and accelerates its ability to absorb CO_2. Figure6 illustrates that the O 1s peak of SnO_2/CNOHHT changed to low bonding energy, showing that SnO_2/CNOHHT has more oxygen deficit sites. Moreover, the N 1s signal and Sn 3d peak in SnO_2/CNOHHT changed with varying binding energies, showing that electrons might be carried from N to Sn. As a result, the highly electron-rich centers of Sn species in SnO_2/CNOHHT facilitate CO_2 adsorption and activation. Furthermore, the electrostatic field generated speeds up charge transfer [13]. These outcomes show that heating the CN substrate with alkali can increase CO_2 electrically reduced through chemical bonds between its active sites and transporters.

Moreover, CO_2-TPD was used to evaluate the CO_2-adsorption and activating properties of catalysts, as shown in

Mingxue Su, et al., J Anal Tech Res 2024
DOI:10.26502/jatr.41

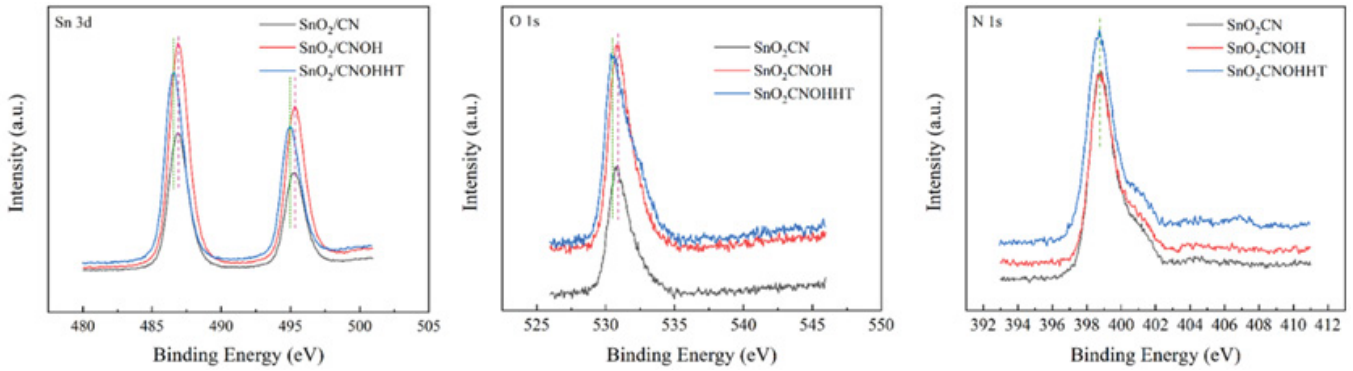

Figure 6: XPS spectra of (a) SnO_2/CN, (b) SnO_2/CNOH and (c) SnO_2/CNOHHT

Table 2: The percentage of all the N variety in each sample

Samples	401.2 eV	399.7 eV	398.5 eV
SnO_2/CN	3.70%	46.00%	50.30%
SnO_2/CNOH	5.90%	47.50%	46.60%
SnO_2/CNOHHT	7.0% (401.7eV)	44.1% (400.2eV)	48.9% (399.0eV)

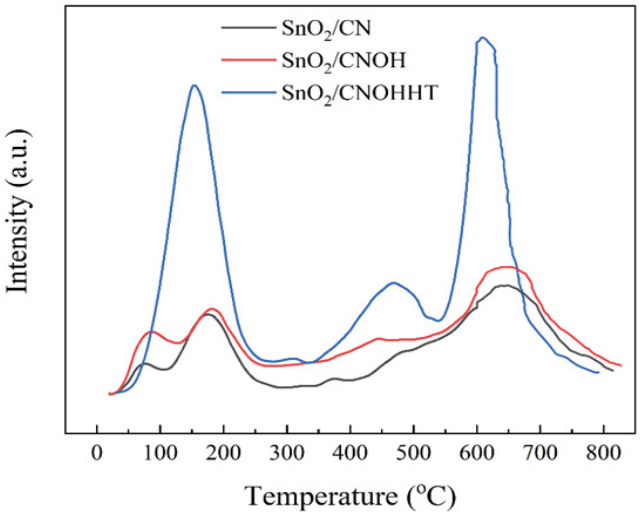

Figure 7: CO_2-TPD profiles of all samples

Table 3: Rate of CO_2 adsorption in each sample

Samples	The CO_2 adsorption amount (mmol/g)
SnO_2/CN	7.69
SnO_2/CNOH	12.04
SnO_2/CNOHHT	48.8

Figure 7. SnO_2/CN and SnO_2/CNOH showed three equivalent CO_2 desorption levels at 95°C, 170°C, and 650°C. Conversely, SnO_2/CNOHHT showed distinct CO_2 desorption levels at 150°C, 470°C, and 620°C. Higher desorption rates often suggest more chemical bonds between the catalyst and CO_2. As a result, SnO_2/CNOHHT exceeded SnO_2/CN and SnO_2/CNOH in terms of both absorption and activity of CO_2. Table 3 highlights the CO_2 adsorption levels of each sample, with SnO_2/CNOHHT having an optimal ability to adsorb at 48.8 mmol/g. In theory, the rate of adsorption should be strongly correlated with the material's particular size and volume of pores. However, Table 1 shows that SnO_2/CNOHHT has the lowest particular surface area and pore size of the samples. The major adsorption ability of SnO_2/CNOHHT is modulated by accessible groups of amino and electron-rich Sn species, consistent with XPS studies.

The electrocatalytic efficiency had originally been assessed using the LSV experiment in a N_2 and CO_2-saturated 0.5 M $KHCO_3$ solution. Compared to the N_2-saturated solution, Figure8a reveals increased current levels for all samples in the CO_2-saturated solution across the investigated potential range, indicating that CO_2RR was more favorable than H_2 evolution reaction (HER). Notably, SnO_2/CNOHHT had the highest level of current (80 mA/cm^2) at -1.87 V (vs. Ag/AgCl). The potential voltages of SnO_2/CN and SnO_2/CNOH have to exceed 2.1 and 1.9 V (vs. Ag/AgCl), respectively, to attain a comparable density of current. Additionally, SnO_2/CNOHHT also showed the lowest onset potential. These results demonstrated the alkali-heat treatment played a positive role in lowering onset potential and increasing current density, and eCO_2RR was more satisfactory to occur on SnO_2/CNOHHT, which was also consistent with the XPS and CO_2-TPD analysis.

Electroreduction processes were carried out utilizing all samples for two hours in a CO_2-saturated 0.5 M $KHCO_3$ solution at a constant potential (-1.5 V vs. Ag/AgCl) to fully assess catalytic performance. In Figure 8b, after electrolysis, the foremost products for all catalysts were CO, H_2, and HCOOH. Furthermore, compared to 62.7% and 81.8% for SnO_2/CN and SnO_2/CNOH, SnO_2/CNOHHT had the highest FE for formic acid among the three catalysts, reaching 90.5%. Notably, the faradaic efficiency of hydrogen (FEH_2) on SnO_2/CNOHHT was much lower than that of the other two

Mingxue Su, et al., J Anal Tech Res 2024
DOI:10.26502/jatr.41

catalysts. The results indicate that after alkali-heat therapy, the displayed surface amino bonds of the CN substrate and highly electron-rich centers of Sn species could inhibit the hydrogen evolution reaction (HER) and improve HCOOH selectivity via enhanced CO_2 adsorption and stimulation features. The FE of CO did not exhibit apparent changes among all the samples, indicating the absence of a competitive relationship between the evolution of carbon monoxide (CO) and the intended production of HCOOH.

To evaluate the reaction kinetics for eCO_2RR, Tafel slopes of all samples were studied and shown in Figure 9a. SnO_2/CNOHHT possessed the lowest Tafel slope compared to the SnO_2/CN and SnO_2/CNOH, suggesting the enhancement of reaction kinetics activity for eCO_2RR to HCOOH. The low Tafel slope is useful to reduce CO_2 swiftly with enhancing overpotential. Electrochemical impedance spectroscopy (EIS) was directed at open-circuit voltage to investigate the charge transfer process. As shown in Figure 9b, SnO_2/CNOHHT exhibited the smallest charge transfer resistance (6.2 ohm) compared to the SnO_2/CN (6.8 ohm) and SnO_2/CNOH (8.8 ohm), suggesting its fastest electron transfer rate and reaction kinetics in eCO_2RR [25]. According to the XPS results, alkali-heat treatment effectively enhanced the chemical bonding between SnO_2 and CN, leading to the improvement of overall electronic conductivity, thereby reducing impedance. This ensures improved charge transfer between the active center and CO_2.

Electrochemical stability, another crucial property of the catalyst, was assessed through an electrolytic experiment conducted in a CO_2-saturated 0.5 M $KHCO_3$ solution at -1.5 V (vs. Ag/AgCl). The current-time relationship for SnO_2/CNOHHT, depicted in Figure 10, revealed a consistent current

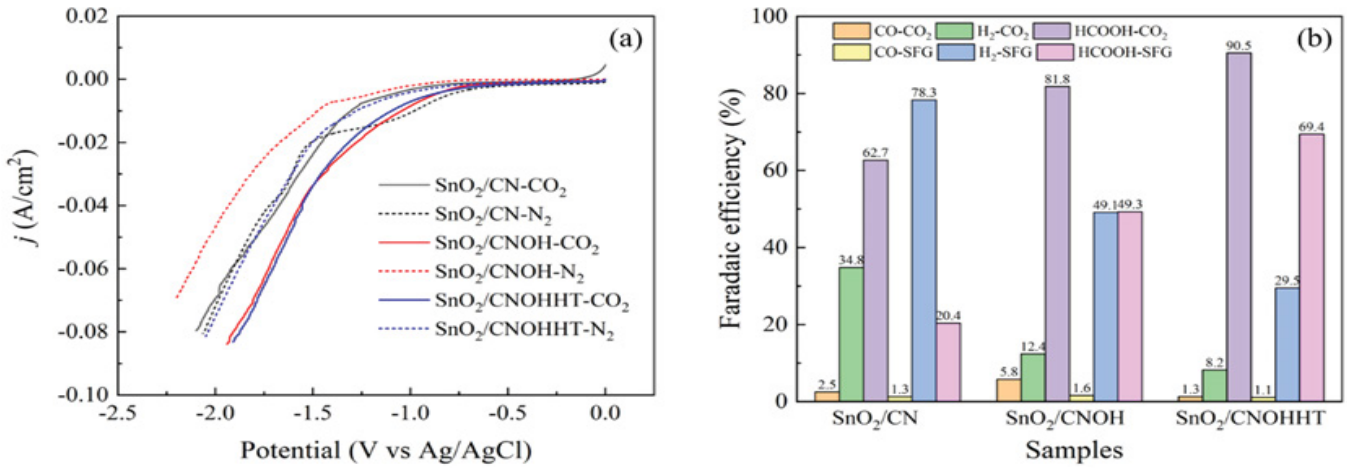

Figure 8: (a) LSV curves of the electrodes in N_2- and CO_2-saturated 0.5 M $KHCO_3$ electrolytes at a scan rate of 50 mV/s and (b) FE of HCOOH, CO, and H_2 at the potential -1.5 V vs. Ag/AgCl after 2 h of eCO_2RR

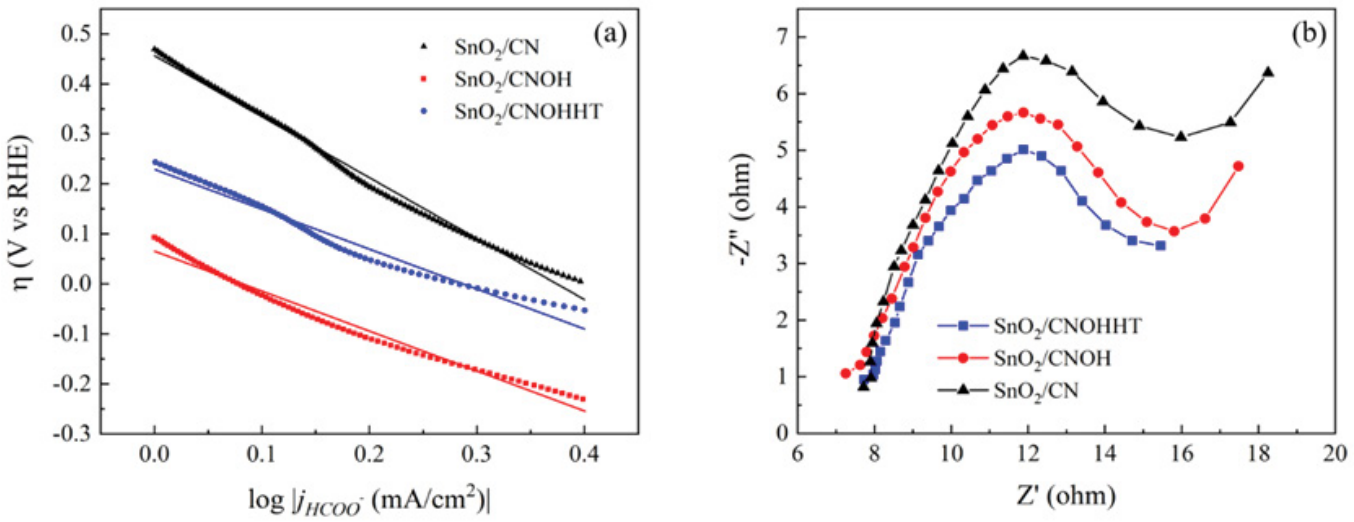

Figure 9: (a) Tafel plots and (b) EIS Nyquist plots of all samples in CO_2-saturated 0.5 M $KHCO_3$ solution

Citation: Mingxue Su, Zhenguo Guo, Ning Li and Bing Zhu. Enhanced Oxygen Tolerance in CO2 Electroreduction to Formic Acid on SnO2/CN Catalyst through Alkali-Heat Treatment. Journal of Analytical Techniques and Research. 6 (2024): 19-27.

Mingxue Su, et al., J Anal Tech Res 2024
DOI:10.26502/jatr.41

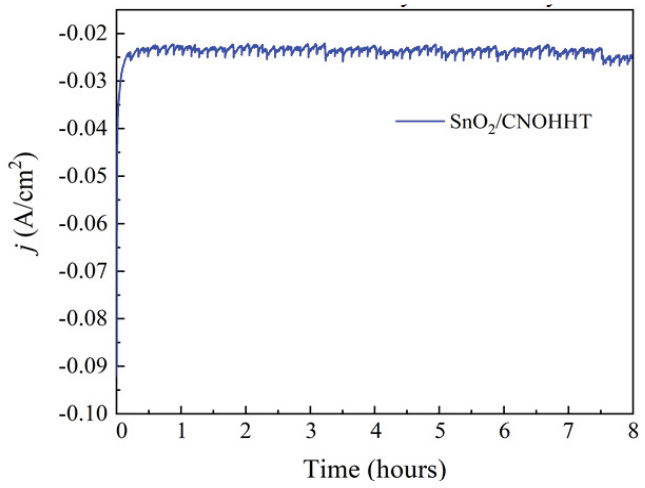

Figure 10: Stability test of all samples at the potential -1.5 V vs. Ag/AgCl

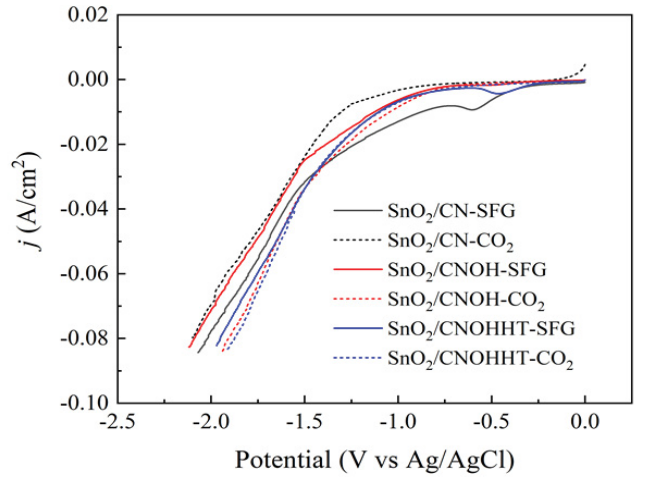

Figure 11: LSV curves of the electrodes in SFG at a scan rate of 50 mV/s

value of 23.5 mA/cm^2 for 8 hours. This result underscores the electrochemical stability of each catalyst.

To further understand the impact of alkali-heat therapy, all catalysts' electroreduction efficiency was evaluated in an SIEG scenario. Figure 11 shows LSV curves for electrodes in SIEG at a scanning pace of 50 mV/s. As seen in Figure 11, when contrasted to pure CO_2 flow, the density of all catalysts decreased with SIEG. SnO_2/CNOHHT showed the smallest decline in current density. Figure 8b shows that the FE of HCOOH for SnO_2/CNOHHT was 69.4%, higher than SnO_2/CNOH (49.3%) and SnO_2/CN (15.4%). Despite a decline in FE of HCOOH for all samples, SnO_2/CNOHHT had the smallest percentage decrease (23.3%) when compared to SnO_2/CN (75.4%) and SnO_2/CNOH (39.7%).

Multi-component adsorption experiment was conducted to assess the effect of alkali and alkali-heat pretreatment on catalyst CO_2 adsorption capability in SIEG. As illustrated in Figure 12, the CO_2/O_2 separation coefficients for SnO_2/CN, SnO_2/CNOH, and SnO_2/CNOHHT were 0.98, 0.95, and 0.90, respectively. A significant divergence from the separation coefficient of one indicates more segregation of the mixed gas particles. This reveals that, under SIEG conditions, the catalyst with alkali-heat treatment showed efficient adsorption of CO_2 from SIEG.

Conclusion

Both untreated and alkali treated catalysts were outperformed by the alkali-heat treated catalyst, which had a superior faradaic efficiency for formic acid at 90.5% at a -1.5 V voltage (vs. Ag/AgCl). Moreover, the alkali-heat treated catalyst demonstrated electrical stability for up to 8 hours. During electro-reduction of simulated industry exhaust gas, this alkali-heat treated catalyst outperformed the other two catalysts in the present of O_2. The increasing fraction of amino-nitrogen in the carbon nitride carrier

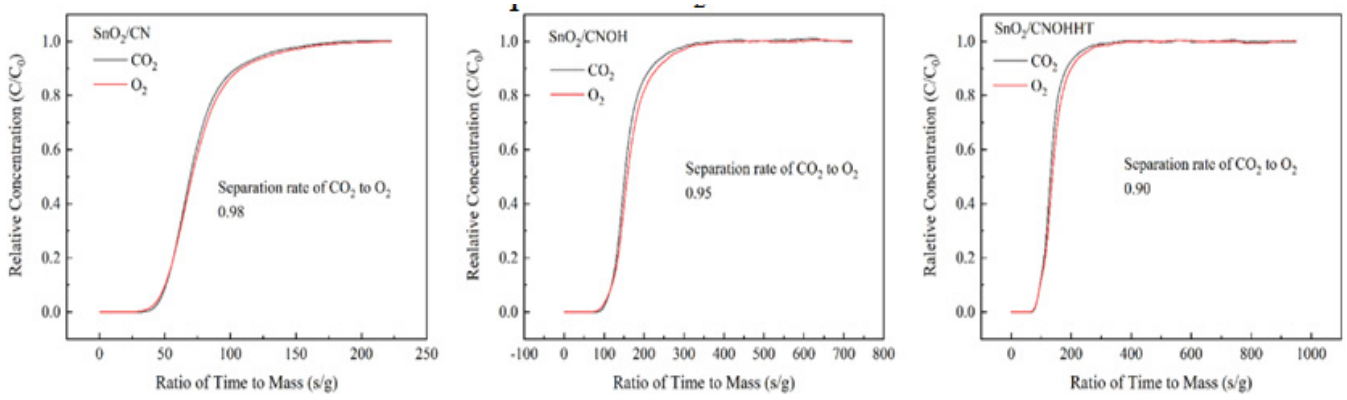

Figure 12: The multi-component competitive adsorption curves of SnO_2/CN (left), SnO_2/CNOH (middle), and SnO_2/CNOHHT (right). Gas condition: 15%CO_2, 8%O_2 and 77%N_2

confirmed the efficiency of alkali-heat pretreatment in terms of the combined catalyst alkalinity and adsorption of CO_2. Furthermore, the treatment strengthened metal-support contacts, increasing the flow of electrons from CN's nitrogen (N) to Sn and creating Sn species with very electron-rich nuclei. It also improved the association between the Sn active site and CO_2, hence activating and reducing CO_2. The raised alkalinity and interaction of the Sn active site with CO_2 enriched from SIEG, improved the oxygen-induced tolerance and electrolytic activity of the composite catalyst during SIEG electro-reduction.

Acknowledgments

The Chinese Ministry of Sciences and Technology of the PRC provided a grant for this research under its National Key Development and Research Program (No. 2020YFC1908704).

Data and code availability

Not Applicable.

Supplementary information

No supplementary materials available.

Ethical approval

Not Applicable.

Conflict of Interests

The authors do not have any financial or other conflicts of interest to declare.

References

1. PP Yang, MR Gao. Enrichment of reactants and intermediates for electrocatalytic CO_2 reduction. Chem Soc Rev 52 (2023): 4343-4380.
2. D Ewis, M Arsalan, M Khaled, et al. Electrochemical reduction of CO_2 into formate/formic acid: A review of cell design and operation. Sep Purif Technol 316 (2023): 123811.
3. A Somoza-Tornos, OJ Guerra, AM Crow, et al. Process modeling, techno-economic assessment, and life cycle assessment of the electrochemical reduction of CO_2: a review. Iscience 24 (2021): 102813.
4. H Cheng, S Liu, JD Zhang, et al. Surface Nitrogen-Injection Engineering for High Formation Rate of CO_2 Reduction to Formate. Nano Lett 20 (2020): 6097-6103.
5. S Zhang, P Kang, TJ Meyer. Nanostructured Tin Catalysts for Selective Electrochemical Reduction of Carbon Dioxide to Formate. J. Am. Chem. Soc 136 (2014): 1734-1737.
6. XS Wang, WH Wang, JQ Zhang, et al. Carbon sustained SnO_2-Bi_2O_3 hollow nanofibers as Janus catalyst for high-efficiency CO_2 electroreduction. Chem Eng J 426 (2021): 131867.
7. D Sun, W Li, RT Guo, et al. Preparation of N-doped biomass C@SnO_2 composites and its electrochemical performance. Diam Relat Mater 120 (2021): 108674.
8. H Wang, Z Liu, Q Liang, et al. A facile method for preparation of doped-N carbon material based on sisal and application for lead carbon battery. J. Clean. Prod 197 (2018a): 332-338.
9. F Li, Y Huang, C Gao, et al. The enhanced photo-catalytic CO_2 reduction performance of g-C_3N_4 with high selectivity by coupling CoNiSx. Mater Res Bull 144 (2021): 111488.
10. W Yang, L Jia, P Wu, et al. Effect of thermal program on structure–activity relationship of g-C_3N_4 prepared by urea pyrolysis and its application for controllable production of g-C_3N_4. J Solid State Chem 304 (2021): 122545.
11. C Hu, MT Liu, A Sakai, et al. Synergistic effect of Cu and Ru decoration on g-C_3N_4 for electrocatalytic CO_2 reduction. J Ind Eng Chem 115 (2022): 329-338.
12. BB Mulik, BD Bankar, AV Munde, et al. Electrocatalytic and catalytic CO_2 hydrogenation on ZnO/g-C_3N_4 hybrid nanoelectrodes. Appl Surf Sci 538 (2021): 148120.
13. J Tian, M Wang, M Shen, et al. Highly Efficient and Selective CO(2) Electro-Reduction to HCOOH on Sn Particle-Decorated Polymeric Carbon Nitride. ChemSusChem 13 (2020): 6442-6448.
14. KY Tao, K Yuan, W Yang, et al. A template co-pyrolysis strategy towards the increase of amino/imino content within g-C_3N_4 for efficient CO_2 photoreduction. Chem Eng J 455 (2023): 140630.
15. Y Xu, JP Edwards, J Zhong, et al. Oxygen-tolerant electroproduction of C2 products from simulated flue gas. Energ Environ Sci 13 (2020): 554-561.
16. Y Takeda, S Mizuno, R Iwata, et al. Gas-fed liquid-covered electrodes used for electrochemical reduction of dilute CO_2 in a flue gas. J CO_2 Util 71 (2023): 102472.
17. N Meng, C Liu, Y Liu, et al. Efficient Electrosynthesis of Syngas with Tunable CO/H_2 Ratios over ZnxCd1-xS-Amine Inorganic-Organic Hybrids. Angew Chem Int Edit 58 (2019): 18908-18912.
18. PS Li, X Lu, ZS Wu, et al. Acid-Base Interaction Enhancing Oxygen Tolerance in Electrocatalytic Carbon Dioxide Reduction. Angew Chem Int Edit 59 (2020): 10918-10923.
19. X Chen, J Chen, NM Alghoraibi, et al. Electrochemical

Mingxue Su, et al., J Anal Tech Res 2024
DOI:10.26502/jatr.41

CO2-to-ethylene conversion on polyamine-incorporated Cu electrodes. Nat Catal 4 (2021): 20-27.

20. Z Sun, JMTA Fischer, Q Li, et al. Enhanced CO_2 photocatalytic reduction on alkali-decorated graphitic carbon nitride. Appl Catal B-Environ 216 (2017): 146-155.

21. H Zhang, T Ouyang, J Li, et al. Dual 2D CuSe/g-C_3N_4 heterostructure for boosting electrocatalytic reduction of CO_2. Electrochim Acta 390 (2021a): 138766.

22. HJ Wang, GW Jiang, XJ Tan, et al. Simple preparation of SnO_2/C nanocomposites for lithium ion battery anode. Inorg Chem Commun 95 (2018b): 67-72.

23. X Li, X Sun, L Zhang, et al. Efficient photocatalytic fixation of N_2 by KOH-treated g-C_3N_4. J Mater Chem A 6 (2018): 3005-3011.

24. Y Shang, Y Ding, P Zhang, et al. Pyrrolic N or pyridinic N: The active center of N-doped carbon for CO_2 reduction. Chinese J Catal 43 (2022): 2405-2413.

25. BH Zhang, S Chen, BR Wulan, et al. Surface modification of SnO_2 nanosheets via ultrathin N-doped carbon layers for improving CO_2 electrocatalytic reduction. Chem Eng J 421 (2021b): 130003.